



EUROPEAN  
COMMISSION

European  
Research Area

# Carbon-14 Source Term

## CAST



## Annual Progress Report on corrosion test (D3.12)

Author(s):

**Frank Druyts (SCK.CEN), Viktor Jobbágy (SCK.CEN), David Bottomley (JRC-ITU), Manuela Fulger (RATEN ICN), Crina Bucur (RATEN ICN), Tomofumi Sakuragi (RWMC)**

Date of issue of this report: 22/11/2016

<b>The project has received funding from the European Union's Seventh Framework Programme for research, technological development and demonstration under grant agreement no. 604779, the CAST project</b>		
<b>Dissemination Level</b>		
<b>PU</b>	Public	<b>x</b>
<b>RE</b>	Restricted to the partners of the CAST project	
<b>CO</b>	Confidential, only for specific distribution list defined on this document	

## **CAST – Project Overview**

The CAST project (CArbon-14 Source Term) aims to develop understanding of the potential release mechanisms of carbon-14 from radioactive waste materials under conditions relevant to waste packaging and disposal to underground geological disposal facilities. The project focuses on the release of carbon-14 as dissolved and gaseous species from irradiated metals (steels, Zircalloys), irradiated graphite and from ion-exchange materials.

The CAST consortium brings together 33 partners with a range of skills and competencies in the management of radioactive wastes containing carbon-14, geological disposal research, safety case development and experimental work on gas generation. The consortium consists of national waste management organisations, research institutes, universities and commercial organisations.

The objectives of the CAST project are to gain new scientific understanding of the rate of release of carbon-14 from the corrosion of irradiated steels and Zircalloys and from the leaching of ion-exchange resins and irradiated graphites under geological disposal conditions, its speciation and how these relate to carbon-14 inventory and aqueous conditions. These results will be evaluated in the context of national safety assessments and disseminated to interested stakeholders. The new understanding should be of relevance to national safety assessment stakeholders and will also provide an opportunity for training for early career researchers.

For more information, please visit the CAST website at:

<http://www.projectcast.eu>

*CAST*  
*Annual Progress Report on corrosion test (D3.12)*

<b>CAST</b>		
Work Package: 3	CAST Document no. :	Document type:
Task: 3.3	CAST-2016-D3.12	R = report
Issued by: SCK.CEN		Document status:
Internal no. : 2016/FDr/Pub-21		Final

Document title
3 rd year Annual Progress Report on corrosion test (D3.12)

## Executive Summary

This report describes the progress made at JRC/ITU, RATEN ICN, RWMC and SCK•CEN for the work on the corrosion of irradiated and unirradiated Zircaloy in the framework of Work Package 3 of the CAST project.

RATEN ICN launched leaching tests in NaOH solution pH12 on irradiated and unirradiated CANDU Zircaloy-4. For the test on irradiated Zircaloy, the first sampling will be performed after 6 months of exposure. The corrosion rate will be determined from electrochemical measurements.

JRC-ITU described the experimental setup related to the leaching test with irradiated Zircaloy-4, planned to start by the end of 2016. The corrosion rates determination will be based on Co-60 (gamma-spec) measurement.

RWMC carried out corrosion measurements on unirradiated zirconium in pure water at low temperatures ranging from 30°C to 80°C. The corrosion rates were determined from hydrogen measurements by the glass ampoule method.

SCK.CEN performed metallographic analysis on unirradiated Zircaloy-4, indicating that most of the precipitates in the metal are Laves phase. The second type of precipitates consist of ZrC, and is elongated, needle-shaped. Furthermore, static and polarised corrosion test setups were designed. First accelerated tests show a broad passive behaviour of Zircaloy-4.

## List of Contents

Executive Summary	iii
List of Contents	v
1 Work at JRC/ITU	6
1.1 Samples	6
1.2 Leaching tests	7
1.2.1 Autoclave	7
1.2.2 Planning	8
2 Work at RATEN ICN	9
2.1.1 Materials	9
2.1.2 Leaching tests and corrosion rate measurements on irradiated Zy-4 samples	10
3 Work at RWMC	11
3.1 Introduction	11
3.2 Hydrogen measurement for unirradiated materials by glass ampoule method	12
3.2.1 Experimental setup	12
3.2.2 Results	13
3.3 Acknowledgement	14
4 Work at SCK.CEN	15
4.1 Introduction	15
4.2 Materials	15
4.3 Metallography	15
4.3.1.1 Sample preparation	16
4.3.1.2 Grain size determination	17
4.3.1.3 Metallographic analysis	17
4.4 Corrosion testing	23
4.4.1 Static tests	23
4.4.2 Polarised corrosion test	24
4.5 Gas chromatography	26
4.6 Future work	26
References	27

## 1 Work at JRC/ITU

### 1.1 Samples

Samples have been cut as 3mm long rings (1-0.5g). The Zircaloy-4 cladding has been defueled. 4 Zircaloy samples were cut at fuel height from the upper end of the rod. The fuel has been pressed out with a die, followed by HNO<sub>3</sub> immersion to remove the remaining fuel (2x 15 min. in 8M HNO<sub>3</sub>) and rinsed. This is followed by a final ultrasonic clean in distilled water for 15mins then finally drying in air. The resulting inner metallic surface appears to be clean and to have a bluish hue (see Figure 1). A similar procedure will be used for the stainless steel samples to be studied in Work Package 2.

The samples were weighed and the dose rates measured. Three of the samples are listed below: specimens 1 and 2 will be the first to be tested.

No.	Specimen	Sample length	Sample weights	Activity (direct contact) mSv.h <sup>-1</sup>
1	13D02-732-2	2mm	0.2656g	33mSv.h <sup>-1</sup>
2	13D02-732-3/2	2mm	0.2714g	42mSv.h <sup>-1</sup>
3	13D02-732-3	1.5mm	0.3798g	222mSv.h <sup>-1</sup>

Gamma spectroscopy measurements will be made on the samples and solutions after the leach tests; this will be used to determine the corrosion rates. The Co-60 count rate is expected to be the best parameter to estimate the corrosion rate.



Figure 1(left): Dark film on inner surface seen after the first acid cleaning. Little difference is seen after the second acid cleaning; (right): pieces of fuel after defueling.

## 1.2 Leaching tests

### 1.2.1 Autoclave

JRC/ITU will use an existing stainless steel autoclave that has been adapted by replacing the PTFE lining by a PEEK lining (Figure 2). A heating plate & jacket is available (one inside the hot cell and another in reserve) and will be used for the higher temperature test at 80°C. The other tests at 30°C will be effectively at ambient hot cell temperatures. Tests will be of 3 months length with a single sampling (gas & liquid) at the end of the test. The pressure will be 1-2 bars. However it was noted that a gas mouse connection was not sufficiently airtight compared to those from INE, so a gas mouse with an improved connection system (similar to that of INE) was constructed for sufficient airtightness and avoid contamination transfer to the C-14 analytical glove box. New connectors are also being fitted to autoclave and glove box.



Quickfit  
connector needing  
replacement

*Figure 2 Autoclave with gas mouse attached. The connection requires improvement in order to allow optimum sampling and avoid transfer of contamination to the analytical glove box.*

Two new autoclaves have been purchased to perform the non-irradiated testing capable of 10 bar up to 100°C; they have a borosilicate glass base and a PTFE cover with a sampling port. They need an injection/extraction system adding for sampling and transfer to the glove box line. In addition, the purchase of further 150ml (200bar) stainless steel autoclave with PEEK lining is underway in order to increase the capacity for testing for the irradiated cladding samples.

### 1.2.2 Planning

There are no test results to report as testing is just about to start shortly. The first 3 month leach testing is due to start in October 2016 and the second sample will be tested in the second autoclave in November 2016. The Zircaloy-4 samples should be taken from the 2 autoclaves after 3 months (ie Jan. 2017 and Feb. 2017) for corrosion measurements in 0.1M NaOH (pH 12) and distilled water, followed by C-14 analyses. The next pair of tests should be finished by April and June 2017 respectively.

## 2 Work at RATEN ICN

### 2.1.1 Materials

The leaching tests started respectively in April 2016 and June 2016 for the irradiated samples and un-irradiated samples.

6 samples of irradiated Zy-4 were available for the leaching tests. These samples were obtained from a CANDU spent fuel bundle that was irradiated for 1 year in the Cernavoda NPP Unit 2 and kept for cooling 4 more years in the Spent Fuel cooling bay. After the cooling period, the fuel bundle was transported to RATEN ICN for different investigations and in the last 2 years it was stored in the ICN hot cells.

Preliminary scanning electron microscopy (SEM) investigations on the CANDU spent fuel were performed. The thickness of the zirconium oxide layer measured along the fuel tube was between 3  $\mu\text{m}$  and 3.5  $\mu\text{m}$ .

To be able to correlate the C-14 content with the Co-60 content, gamma measurements were carried out on the samples before starting the leaching tests. Gamma scanning will also be performed to measure the Co-60 content in the leachate solution.

Due to the high content of Cs-137 in the irradiated Zy-4 samples, gamma measurements were performed on small rings cut from the irradiated Zy-4 to be used in the long term leaching tests. An ORTEC Gamma spectrometer with HPGe detector was used for these measurements and results are reported as Bq per gram of irradiated Zy-4 as presented in Table 1. Figure 3 presents a spectrum showing the main gamma emitters.

Table 1 Main gamma emitters identified in the irradiated Zy-4

<b>Radionuclide</b>	<b>Co-60</b>	<b>Cs-137</b>	<b>Cs-134</b>	<b>Sb-125</b>
Activity [Bq/g]	1.601 E+05	5.4895 E+06	5.676 E+05	6.193 E+06



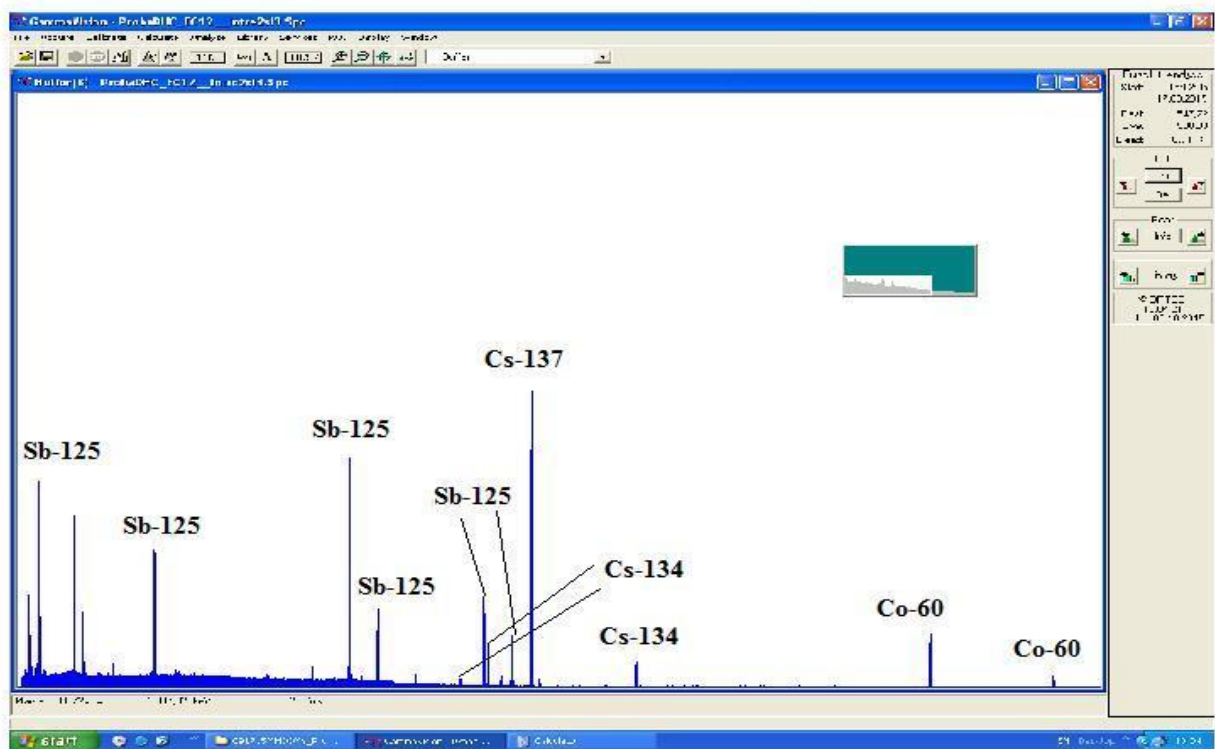


Figure 3 Spectrum with the main gamma emitters

Each of the six samples, available for the experimental programme proposed under CAST, was cut in two pieces: a small one for C-14 measurement and a larger one to be immersed in deaerated NaOH solution (pH ~ 12).

### 2.1.2 Leaching tests and corrosion rate measurements on irradiated Zy-4 samples

The leaching test has been run under  $N_2$  atmosphere. Six glass tubes were adapted to allow monthly  $N_2$  purging in order to ensure continuous anoxic conditions (Figure 4). Gaseous C-14 will not be analysed. Due to the high radiation dose, the glass tubes were placed inside of a lead castle.

After 6 months (by October 2016), the first two leachates will be sampled. More sampling will be carried out later. The solution will be analysed to determine C-14 contents.

Furthermore, electrochemical tests will be carried out mid–November on the two irradiated Zy-4 samples to determine the corrosion rate. The experimental setup consists of an

AUTOLAB 302 electrical potentiostat/galvanostat connected to an electrochemical cell glass cell equipped with a Pt counter electrode, an Ag/AgCl reference electrode and the Zy-4 working electrode.



Figure 4 View of the six glass bottles used in the leaching tests

### 3 Work at RWMC

#### 3.1 Introduction

In 2016, RWMC has launched experiment on unirradiated zirconium in pure water. The D3.10 deliverable (Jobaggy, 2015) reports all the previous work on corrosion performed by RWMC. It includes corrosion rate measurements in alkaline solutions for both irradiated and unirradiated Zircaloy. Different techniques were applied: hydrogen measurements by gas flow method and glass ampoule method for unirradiated Zircaloy and release rate calculations for irradiated Zircaloy. In this report, an update is given on the corrosion work performed in pure water.

## 3.2 Hydrogen measurement for unirradiated materials by glass ampoule method

### 3.2.1 Experimental setup

Zirconium, Zircaloy-2 and Zircaloy-4 were obtained from CEZUS Co., Ltd. The samples were pretreated to produce an appropriate thickness by undergoing two sets of cold-rolling, followed by vacuum annealing after each set to remove the hydrogen absorbed during cold-rolling. The final polishing was done with 0.02 mm alumina powder. Zircaloy or pure zirconium 23 strips (21 pieces; 3 mm×90 mm×0.1 mm, 2 pieces; 3 mm×90 mm×0.05 mm) were placed in a glass ampoule. The outline for test procedure is shown in Figure 5. A stop-cock was attached, then the ampoule was filled with the appropriate solution and the stop-cock closed. This enclosure procedure was performed in a glove box that had been purged by nitrogen gas with oxygen concentration below 0.1 ppm. The ampoules were moved outside the glove box and sealed by heating. After corrosion, the ampoules were set on the vacuum gas collecting system connected with a gas chromatography (YANACO G-2800) and hydrogen gas was measured. The hydrogen absorbed into the metal was also measured by an inert gas melting system together with gas chromatography (LECO RH-404).

In the ampoule method, the corrosion rate,  $R_c$  ( $\mu\text{m}/\text{y}$ ), is obtained from the following equation (1) based on the oxidation and hydriding reaction under stoichiometry.

$$R_c = \frac{(A_{gas} + 3 \cdot A_{abs}) \cdot M_{Zr}}{4 \cdot \rho \cdot t} \cdot 10^6 \quad (1)$$

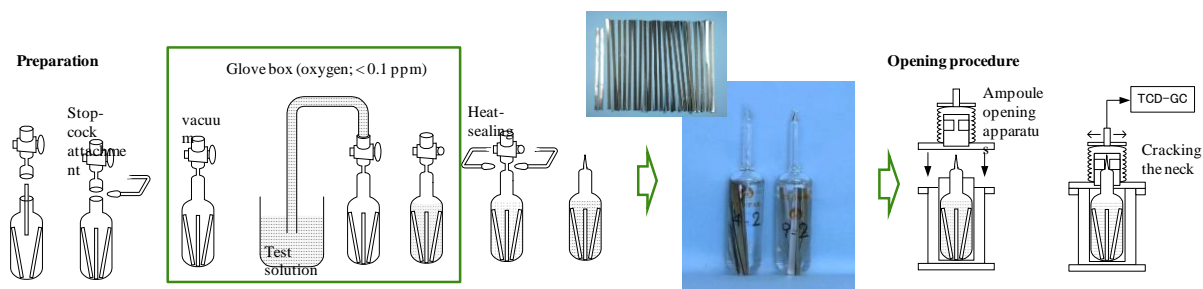


Figure 5 Procedure for ampoule batch corrosion experiment.

### 3.2.2 Results

The results on the corrosion rates in pure water as well as in alkaline solutions are shown in Figure 6. The data for gas flow experiments are obtained from (Sakuragi et al. 2013). A part of the ampoule test (Kato et al., 2014) and BWR data (Yamashita, et al., 2014) can be found in the literature. The PWR data are obtained from the work of (Yamaguchi et al. 1999).

In the hydrogen measurements from unirradiated Zircaloy and pure zirconium, the corrosion rate decreases with time. Detailed analysis of the gas flow experiment data has found that the corrosion kinetics are represented by the parabolic rate law (Sakuragi, et al., 2013). This kinetic result differs from the general out-pile (high temperature) corrosion behaviour of the cubic rate law. The corrosion rate increases as the temperature increases. The difference between Zircaloy-2 and Zircaloy-4 is negligible. In comparison with the case of pure water it is possible that the solution components and increased pH slightly enhance the corrosion rate. However, the difference between Zircaloy-4 and pure zirconium in pure water is also negligible.

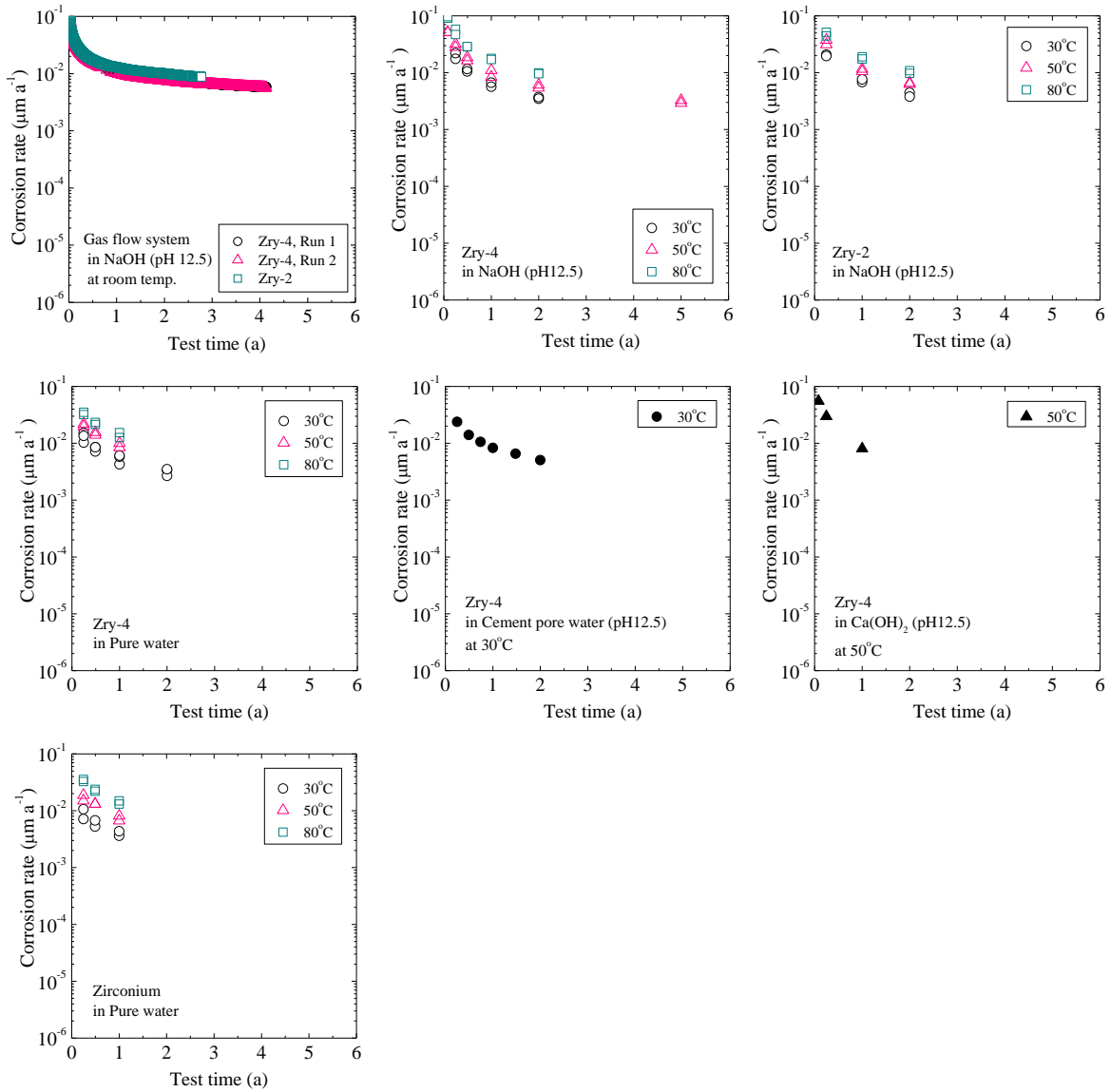


Figure 6 Corrosion rate for zirconium materials.

### 3.3 Acknowledgement

This research is a part of the “Research and development of processing and disposal technique for TRU waste (FY2015)” program funded by Agency for Natural Resources and Energy, Ministry of Economy, Trade and Industry of Japan.

## 4 Work at SCK.CEN

### 4.1 Introduction

The aim of the work at SCK•CEN is to investigate the release of  $^{14}\text{C}$  from Zircaloy-4 claddings representative for Belgian PWR claddings and the  $^{14}\text{C}$  speciation in a cementitious environment, which is relevant for the Belgian Supercontainer design, as perceived for the geological disposal of high level waste. In order to achieve this, SCK.CEN has designed both static and accelerated corrosion tests to perform on irradiated material representative of commercial fuel cladding. This report describes the samples (both non-irradiated and irradiated), metallography of the non-irradiated samples, corrosion set-up for the static and accelerated tests, gas chromatography (GC) system for identification and quantification of the  $^{14}\text{C}$  species, and the remaining work. Previous work has been described in D3.4 and D3.10.

### 4.2 Materials

Two types of Zircaloy-4 samples were obtained for testing: non-irradiated and irradiated. The unirradiated material had a measured composition of 1.30 wt% Sn, 0.20 wt.% Fe, 0.10 wt.% Cr, and 0.14 wt.% O, while the balance was Zirconium. This was obtained as a 98 mm long rod with a diameter of 12 mm, from which samples were cut for accelerated testing with a length of 3 mm. A steel wire conductor was connected to the back of each sample with Circuitworks® conductive epoxy, which is a two-part hardening epoxy resin. After cutting, the samples were cold-embedded with SpeciFix® resin.

The irradiated Zircaloy samples underwent a fluence of  $1.0 \text{ E } 21 \text{ n/cm}^2$  ( $E > 1 \text{ MeV}$ ). The cladding tube was cut into 3 pieces with a length of 20 mm each, an external diameter of 9.6 mm and a wall thickness of 1.2 mm, which will be used for static tests.  $\gamma$ -ray spectroscopy will be carried out in August 2016 on an additional piece of irradiated cladding.

### 4.3 Metallography

Metallographic investigation was carried out on the unirradiated samples only.

Metallographic analysis is planned in August/September 2016 for the irradiated material.

#### 4.3.1.1 Sample preparation

A slice of about 0.6 mm thick was cut from the Zry-4 rod with a Struers Accutom 50 instrument. This slice was mechanically polished on SiC paper (500, 1200 and 4000). When the thickness of the slice was reduced below 0.3 mm, five discs of 3 mm in diameter were punched out of the slice. These discs were polished further on SiC paper until the thickness was reduced to 0.1 mm.

The final step in the sample preparation was electrochemical double jet polishing with a Struers Tenupol-3 instrument. The electrolyte used consisted of 5% perchloric acid and 95% methanol. To polish Zircaloy, the temperature of the electrolyte was reduced to -30 °C and a voltage of 25V was applied. Two samples were polished until perforation and one sample was only polished for 10s. The last two samples were held in reserve.

The first two samples (polished until perforation) were used for the TEM investigation in a JEOL 3010 microscope operating at 300 kV. Bright field, dark field and selected area electron diffraction were used to determine the defect structure and precipitates. Energy dispersive X-ray spectroscopy (EDS) was applied for the qualitative determination of the composition of the precipitates. It should be noted that during the EDS measurement a small amount of carbon is deposited on the surface of the sample. Moreover, when analysing small precipitates, a part of the signal is generated in the steel adjacent, or around (on top or below) the precipitate. Therefore, it is not possible to get a quantitative composition of the observed precipitates and carbides, but qualitative statements are possible.

The latter samples (polished for 10 s during the final polishing step) were used in the SEM investigation for the determination of the grain size. Even though the polishing conditions may not be optimal to reveal the grain structure, it was possible to determine the grain structure under the electron beam of the SEM. The best results were obtained in the back-scattered electron (BSE) images, where the contrast is mainly induced by the atomic weight. Light elements scatter fewer electrons than heavy elements and are darker in the BSE images.

#### 4.3.1.2 Grain size determination

The grain size of each material was determined from the BSE images of the samples after electrochemical polishing for 10s. The grain size is determined in accordance with the ASTM standard E112-95. The grain size number (G) is defined as:

$$N = 2^{G-1}$$

Where,  $N$  is the number of grains per inch<sup>2</sup> at a magnification of 100× which equals the number of grains per mm<sup>2</sup> at a magnification of 1× divided by 15.50.

This number is obtained by placing a circle of known diameter on the BSE images and by counting the number of grains within the circle. The grains that intersect the circle count for half a grain. The SEM images calibrating the actual diameter of the circle can be determined and the average grain size calculated. This value is used to calculate the number of grains per mm<sup>2</sup> and the grain size number.

#### 4.3.1.3 Metallographic analysis

According to the specifications, Zircaloy-4 consists of about 98 wt% Zr, 1.2-1.7 wt% Sn, 0.18-0.24 wt% Fe, 0.07-0.13 wt% Cr and 1100-1400 ppm O. The Sn is uniformly distributed over the bulk material, but Fe and Cr are concentrated in Zr(Fe,Cr)<sub>2</sub> intermetallic Laves phases. Carbon has a weakly unfavourable effect on corrosion behaviour and the amount of carbon is limited to a maximum of 270 ppm.

The grains structure of Zircaloy-4 is represented in Figure 7. This material consists of small uniform equiaxed grains with a grain size of 11.8, which corresponds to an average grain size of 6 μm with a surface area of 36.4 μm<sup>2</sup>. The small black spots can be attributed to the Laves phases.



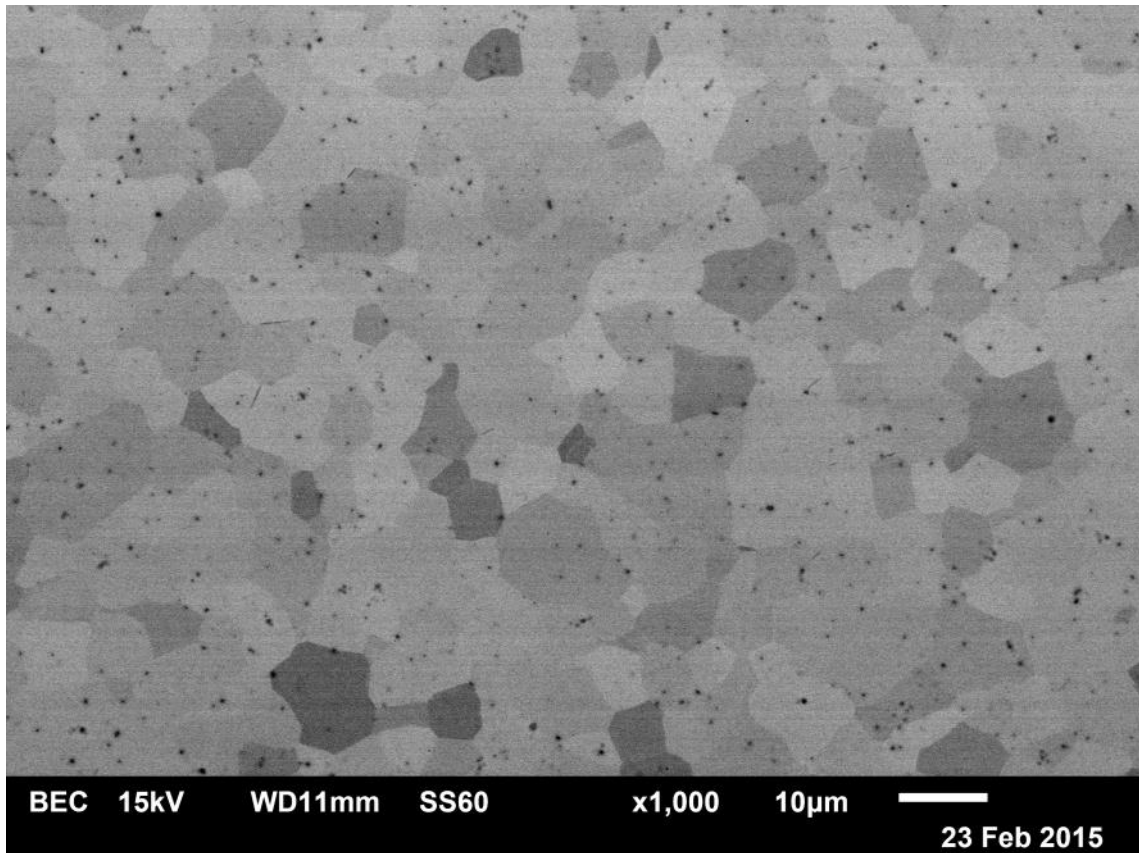


*Figure 7 BSE image revealing the microstructure of Zircaloy-4.*

Typical images of the defect structure of Zircaloy-4 are shown in Figure 8 (top left and top right). The main defects that are occurring are line dislocations with a density of  $4.1 \times 10^{13}/\text{m}^2$ . The grain orientation can be determined from the diffraction pattern as shown in Figure 8 (bottom). It was found that most grains have a comparable orientation, which was identified as the [1-210] zone axis. It is known that during the manufacturing process, the grains become textured, which results in grains having a similar orientation.

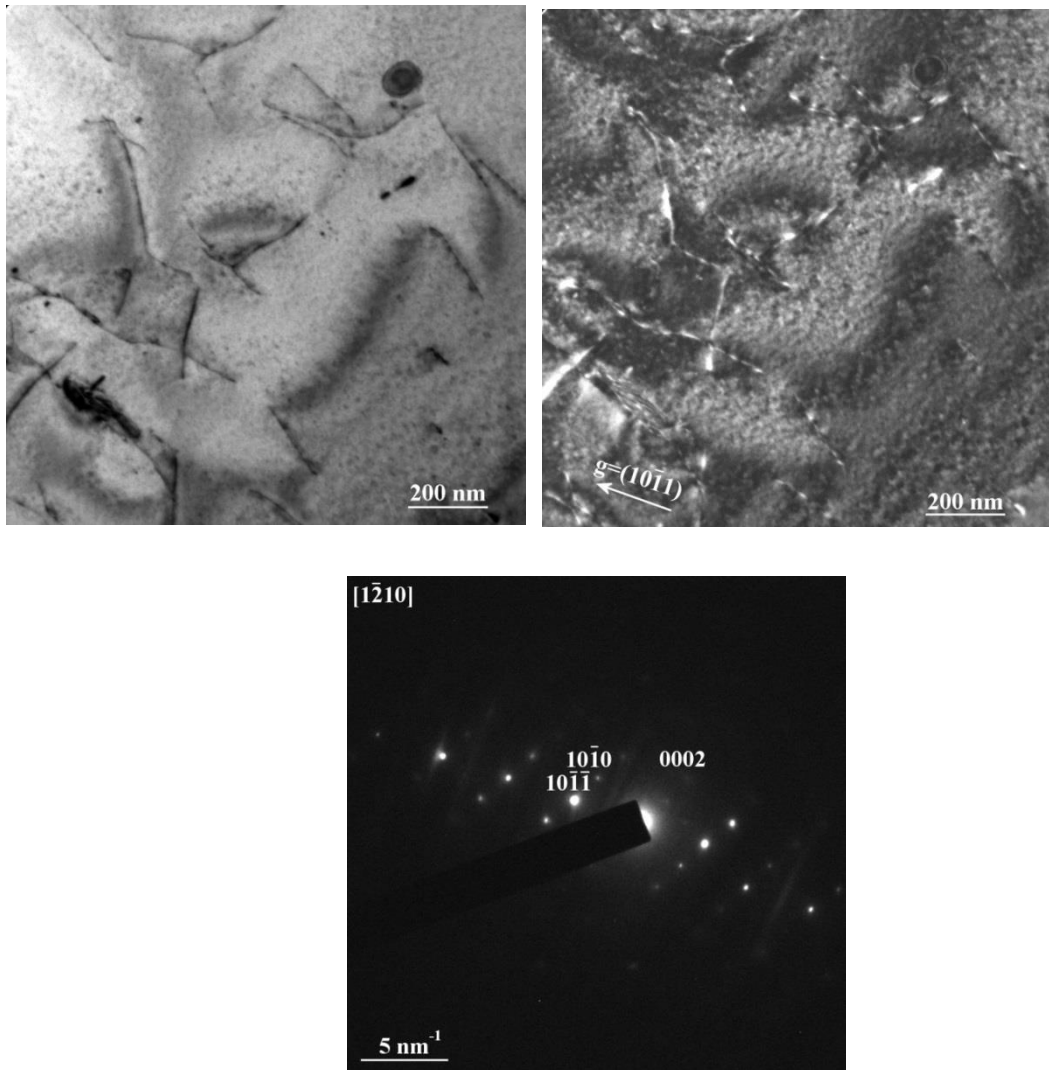


Figure 8 Top left: Bright field; top right: Dark field images of the typical defect structure in Zircaloy-4; bottom: Typical diffraction pattern showing the grain orientation is close to the  $[1\bar{2}10]$  zone axis.

Most of the precipitates present in a Zircaloy-4 material are Laves phases. An example of such a precipitate is given in Figure 9 (top left and right). The electrochemical polishing process dissolves partially these precipitates. This can be seen with the upper right part of the precipitate, which has a higher intensity (less absorption) and therefore shows no diffraction contrast.

The nominal composition of this phase is  $\text{Zr}(\text{Fe,Cr})_2$ . The composition is confirmed by the EDS analysis on this particle, which is shown in Figure 9 (bottom). Apart from the Zr signal, peaks corresponding to Fe and Cr were observed as well. Any carbon observed in other samples is considered to be the result of a surface contamination during the analysis because it is not present in this sample.

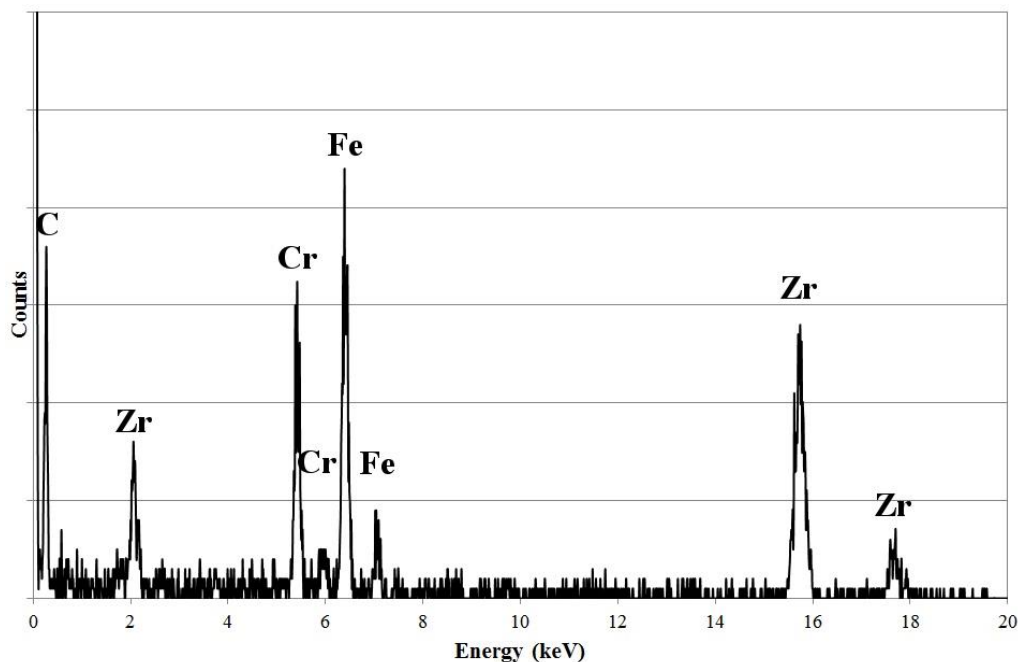
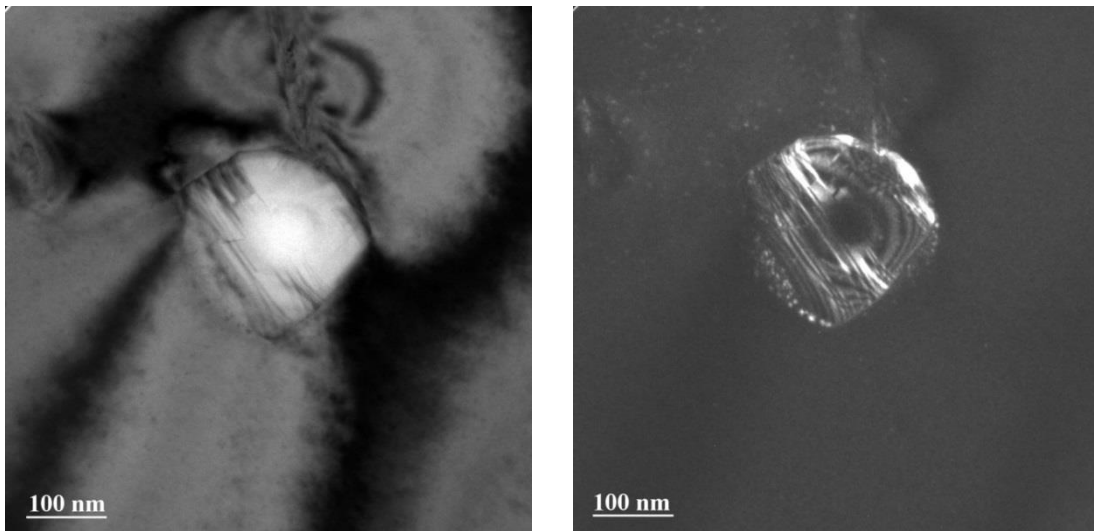
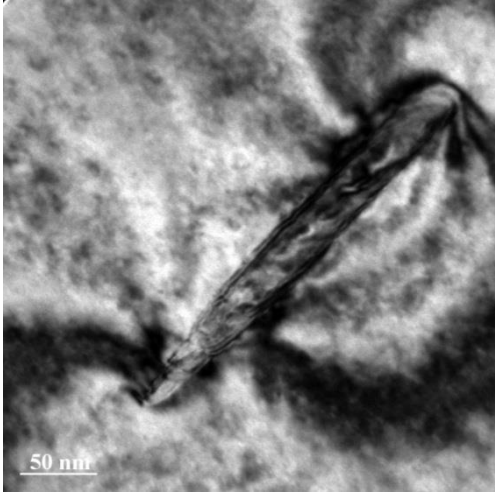


Figure 9 Top left: Bright field, top right: Dark field image of Laves phase in Zircaloy 4; bottom: The corresponding EDS spectrum confirming the  $\text{Zr}(\text{Fe,Cr})_2$  composition.

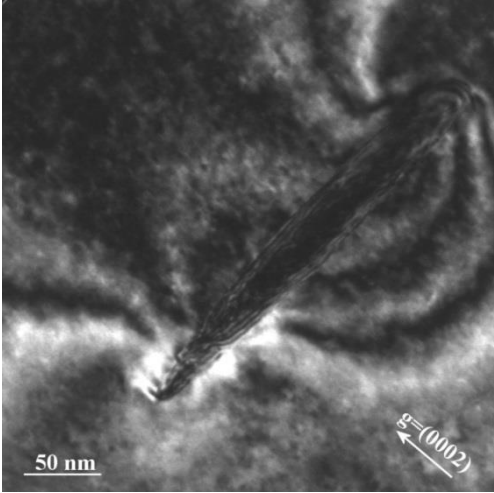
A second type of precipitate is shown in Figure 10a), b) and c). The bright field and dark field images show that these precipitates are elongated along the (0002) planes and are needle or platelet shaped. The EDS spectrum in Figure 10e) shows the composition of the precipitate in comparison to the spectrum of the bulk Zry-4. For the visual comparison of Figure 9 (bottom) and Figure 10 e), the spectrum of the precipitate is renormalized so that both spectra have the same total number of counts. The bulk metal consists mainly of zirconium. Small amounts of carbon and oxygen are detected as well, which can be attributed to the expected contamination of the surface as well as slight oxidation of the zirconium which is very reactive. When magnifying the spectrum between 2 and 6 keV, a small Sn peak can be found, in agreement with the 1.2wt% of Sn added to the Zry-4. No Cr or Fe can be detected as these elements are forming the Laves phases. The spectrum of the precipitate (Figure 10 (bottom)) only contains Zr and C. The carbon content is significantly higher than in the spectrum of the bulk material. This may be the result of higher local contamination during the recording of this spectrum or it can be an indication that carbon is present in the precipitate.

A second option to identify the precipitate is to determine the crystallographic structure from the diffraction pattern shown in Figure 10d). Because of the small size of the precipitate, the appearance of diffraction spots from the bulk Zircaloy could not be avoided and the 0002, -1011 and -1010 reflections, typical for the [1-210] zone, are indicated. The additional reflections agree with the [110] zone axis of a face centered cubic (FCC) structure with a lattice parameter of  $4.6 \pm 0.2 \text{ \AA}$ . Several phases, including ZrC, ZrN or ZrH<sub>2</sub>, were found to have the right crystal structure. In combination with the EDS results, it is most likely that this phase is a ZrC precipitate.

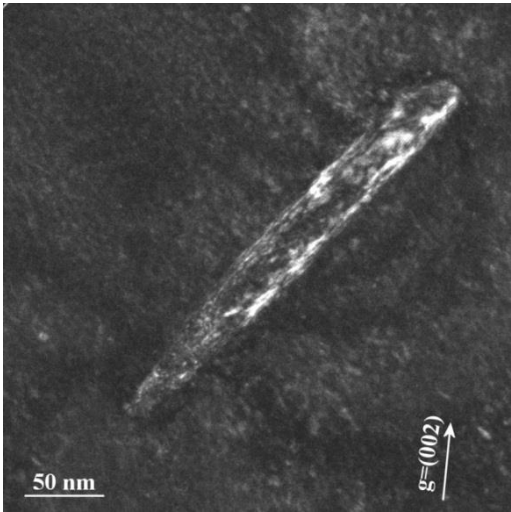
a)



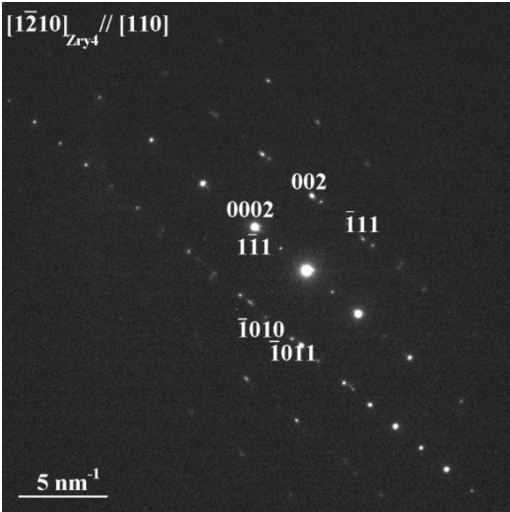
b)



c)



d)





e)

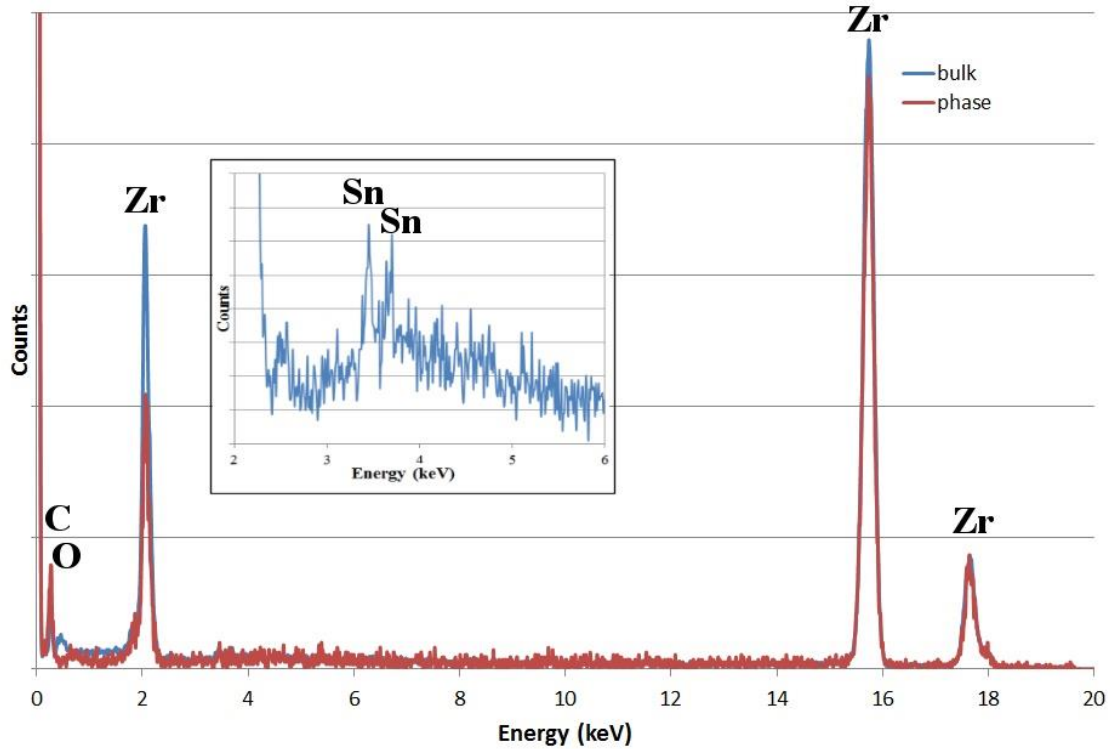


Figure 10a) bright field and b,c) dark field images of a second type precipitate in Zircaloy-4, presumably a ZrC. d) The corresponding diffraction pattern and e) the EDS analysis. The inset shows a magnified part of the bulk metal spectrum, clarifying the presence of Sn peaks.

#### 4.4 Corrosion testing

Two types of corrosion tests have been performed: (i) static corrosion tests to allow for a more realistic corrosion behaviour and associated  $^{14}\text{C}$  release and speciation, and (ii) polarised corrosion tests with applied potential, which mainly serve for preliminary speciation determination.

##### 4.4.1 Static tests

Figure 11 shows the experimental setup of the static corrosion test. It consists mainly of a PEEK-coated steel vessel with an internal volume of 50 cm<sup>3</sup>. The vessel is filled with a

Ca(OH)<sub>2</sub> solution of pH 12.5 and a Zr-4 sample (irradiated or unirradiated) will be immersed. Tests with irradiated Zircaloy-4 are planned to start in August 2016 and will last for 6 months. After 6 months, both liquid and gaseous samples will be sampled for gas chromatography (GC) analysis.

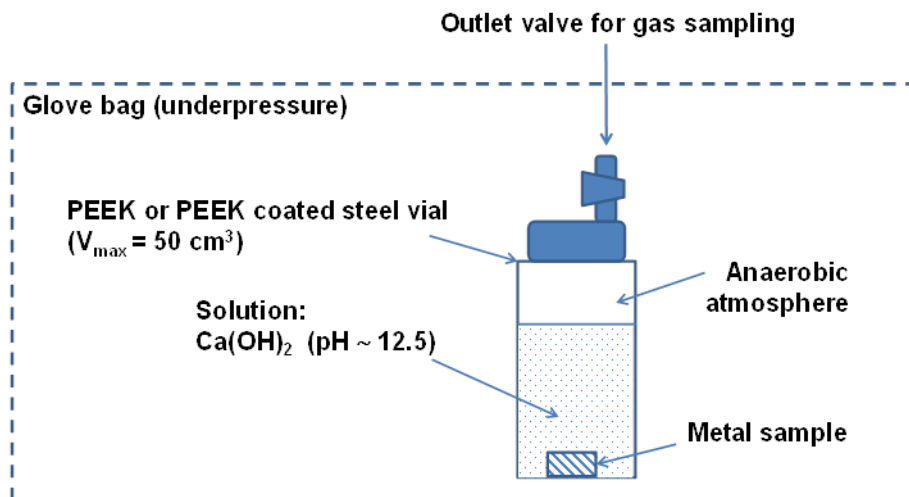


Figure 11 Experimental setup of the static corrosion test

#### 4.4.2 Polarised corrosion test

Figure 12 shows the experimental setup of the polarised corrosion test. A traditional three-electrode setup is used, with the working electrode prepared as described in section 2, a house-made Ag/AgCl reference electrode, and a platina counter electrode. During preliminary tests, potentiodynamic polarization measurements were carried out, during which the potential was scanned from the cathodic to the anodic region and the current was recorded. A typical result (polarization curve) is shown in Figure 13. The polarization curve exhibits a broad passive range.

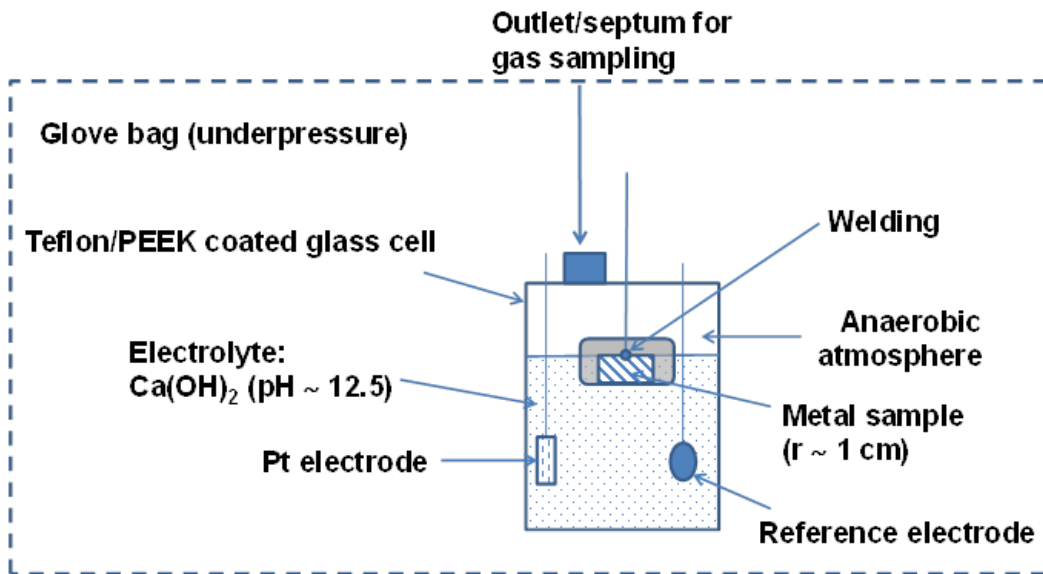


Figure 12 Experimental setup of a polarised corrosion test.

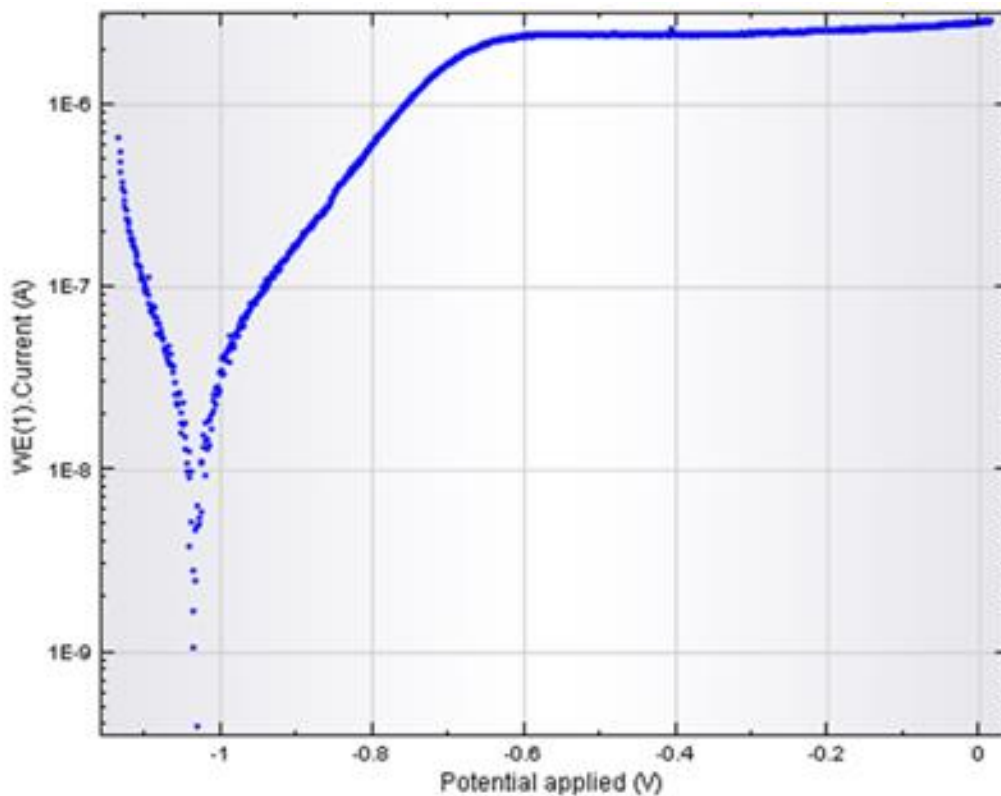


Figure 13 Polarisation curve of (unirradiated) Zircaloy-4 in  $\text{Ca}(\text{OH})_2$  solution at pH 12.5.



## 4.5 Gas chromatography

For the determination of the  $^{14}\text{C}$  speciation, a gas chromatography system will be installed (to be delivered in September 2016). The acquired system is a Shimadzu GC-2010 Plus, which is tailor-made to meet our requirements. Detectors include a Flame Ionization Detector (FID), a Barrier Discharge Ionization Detector (BID), and a Pulse Discharge Helium Ionisation Detector (PDHID). The operation of the FID is based on the detection of ions formed during combustion of organic compounds in a hydrogen flame. The generation of these ions is proportional to the concentration of organic species in the sample gas stream. The response of a FID is semi-universal: all hydrocarbons can be detected. The FID has a detection limit of approximately 1 mg/L. In a BID detector, a plasma is generated by applying a high voltage to a quartz dielectric chamber, in the presence of helium. Compounds that elute from the GC column are ionized by this He plasma, then captured with collection electrodes and described as peaks. The limit of detection of the BID is approximately 500 ng/L. The PDHID uses a stable, low powered, pulsed DC discharge in helium as an ionization sources. Compounds coming from the GC are ionized by photons from the helium discharge and the resulting electrodes are captured in a collector electrode where the current is quantified as the detector output. The limit of detection of the PDHID is approximately 50 ng/L. To determine the total amount of  $^{14}\text{C}$  in the leachate, samples will be taken for liquid scintillation counting.

## 4.6 Future work

SCK.CEN plans the following work in year 4:

- Metallography of the irradiated samples
- $\gamma$ -ray spectrometry of the irradiated Zircaloy-4
- Start-up of the static leaching tests
- Start-up of the accelerated corrosion tests
- Gas and liquid phase analysis with GC, both for the accelerated and static tests
- Final reporting

The final report is expected for 2017.

## References

JOBAGGY, V, 2015. ANNUAL PROGRESS REPORT ON CORROSION (D3.10)

KATO, O, TANABE, H, SAKURAGI, T, NISHIMURA, T, TATEISHI, T. 2014. Corrosion tests of Zircaloy hull waste to confirm applicability of corrosion model and to evaluate influence factors on corrosion rate under geological disposal conditions, In: *Materials Research Society Proceedings*, Vol. 1665, 195-202.

SAKURAGI, T, MIYAKAWA, H, NISHIMURA, T, TATEISHI, T. 2013. Long-term corrosion of Zircaloy-4 and Zircaloy-2 by continuous hydrogen measurement under repository condition, In: *Materials Research Society Proceedings*, Vol. 1518, 173-178.

YAMAGUCHI, T, TANUMA, S, YASUTOMI, I, NAKAYAMA, T, TANABE, H, KATSURAI, K, KAWAMURA, W, MAEDA, K, KITAO, H and SAIGUSA, M. 1999. A Study on Chemical Forms and Migration Behaviour of Radionuclides in Hull Wastes. Radioactive Waste Management and Environmental Remediation, *Proceedings of the ASME 1999 ICEM conference*, September 26-30, Nagoya, Japan, ASME.

YAMASHITA, Y, TANABE, H, SAKURAGI, T, TAKAHASHI, Y, SASOH, M. 2014. C-14 release behavior and chemical species from irradiated hull waste under geological disposal conditions, In: *Materials Research Society Proceedings*, Vol. 1665, 187-194.